BEST AVAILABLE IMAGES

Defective images within this document are accurate representations of the original documents submitted by the applicant.

Defects in the images may include (but are not limited to):

- BLACK BORDERS
- TEXT CUT OFF AT TOP, BOTTOM OR SIDES
- FADED TEXT
- ILLEGIBLE TEXT
- SKEWED/SLANTED IMAGES
- COLORED PHOTOS
- BLACK OR VERY BLACK AND WHITE DARK PHOTOS
- GRAY SCALE DOCUMENTS

IMAGES ARE BEST AVAILABLE COPY.

As rescanning documents *will not* correct images, please do not report the images to the Image Problem Mailbox.

Practitioner's Docket No.: 081468-0306865 **PATENT**
Client Reference No.: P-0393.010-US

IN THE UNITED STATES PATENT AND TRADEMARK OFFICE

In re application of: Confirmation No: 6805

MARTIN LOWISCH, et al.

Application No.: 10/716,939 Group No.: 2812

Filed: November 20, 2003 Examiner:

For: DEVICE MANUFACTURING METHOD AND COMPUTER PROGRAM

Commissioner for Patents
P.O. Box 1450
Alexandria, VA 22313-1450

SUBMISSION OF PRIORITY DOCUMENT

Attached please find the certified copy of the foreign application from which priority is claimed for this case:

Country	Application Number	Filing Date
EUROPE	02258208.4	November 28, 2002

Date: March 26, 2004

PILLSBURY WINTHROP LLP
P.O. Box 10500
McLean, VA 22102
Telephone: (703) 905-2000
Facsimile: (703) 905-2500

Robert C. Perez
Registration No. 39328

Customer Number: 00909

Europäisches Patentamt	European Patent Office	Office européen des brevets

Bescheinigung | Certificate | Attestation

Die angehefteten Unterlagen stimmen mit der ursprünglich eingereichten Fassung der auf dem nächsten Blatt bezeichneten europäischen Patentanmeldung überein.

The attached documents are exact copies of the European patent application described on the following page, as originally filed.

Les documents fixés à cette attestation sont conformes à la version initialement déposée de la demande de brevet européen spécifiée à la page suivante.

Patentanmeldung Nr. | Patent application No. | Demande de brevet n°

02258208.4

Der Präsident des Europäischen Patentamts;
Im Auftrag

For the President of the European Patent Office

Le Président de l'Office européen des brevets
p.o.

R C van Dijk

Europäisches Patentamt | European Patent Office | Office européen des brevets

Anmeldung Nr:
Application no.: 02258208.4
Demande no:

Anmeldetag:
Date of filing: 28.11.02
Date de dépôt:

Anmelder/Applicant(s)/Demandeur(s):

ASML Netherlands B.V.
De Run 1110
5503 LA Veldhoven
PAYS-BAS

Bezeichnung der Erfindung/Title of the invention/Titre de l'invention:
(Falls die Bezeichnung der Erfindung nicht angegeben ist, siehe Beschreibung.
If no title is shown please refer to the description.
Si aucun titre n'est indiqué se referer à la description.)

Device manufacturing method and computer programs

In Anspruch genommene Priorität(en) / Priority(ies) claimed /Priorité(s) revendiquée(s)
Staat/Tag/Aktenzeichen/State/Date/File no./Pays/Date/Numéro de dépôt:

Internationale Patentklassifikation/International Patent Classification/
Classification internationale des brevets:

G03F7/20

Am Anmeldetag benannte Vertragstaaten/Contracting states designated at date of filing/Etats contractants désignées lors du dépôt:

AT BE BG CH CY CZ DE DK EE ES FI FR GB GR IE IT LI LU MC NL PT SE SK TR

Device Manufacturing Method and Computer Programs

The present invention relates to device manufacturing methods comprising the steps of:

- providing a substrate that is at least partially covered by a layer of radiation-sensitive material;
- providing a projection beam of radiation using a radiation system;
- using a reflective mask to endow the projection beam with a pattern in its cross-section;
- projecting the patterned beam of radiation onto a target portion of the layer of radiation-sensitive material,

Such methods can be used, for example, in the manufacture of integrated circuits (ICs) and can be carried out using a lithographic projection apparatus. In such a case, the mask may generate a circuit pattern corresponding to an individual layer of the IC, and this pattern can be imaged onto a target portion (*e.g.* comprising one or more dies) on a substrate (silicon wafer) that has been coated with a layer of radiation-sensitive material (resist). In general, a single wafer will contain a whole network of adjacent target portions that are successively irradiated via the projection system, one at a time. In current apparatus, employing patterning by a mask on a mask table, a distinction can be made between two different types of machine. In one type of lithographic projection apparatus, each target portion is irradiated by exposing the entire mask pattern onto the target portion in one go; such an apparatus is commonly referred to as a wafer stepper. In an alternative apparatus —commonly referred to as a step-and-scan apparatus — each target portion is irradiated by progressively scanning the mask pattern under the projection beam in a given reference direction (the "scanning" direction) while synchronously scanning the substrate table parallel or anti-parallel to this direction; since, in general, the projection system will have a magnification factor M (generally < 1), the speed V at which the substrate table is scanned will be a factor M times that at which the mask table is scanned. More information with regard to lithographic devices as here described can be gleaned, for example, from US

6,046,792, incorporated herein by reference.

In a manufacturing process using a lithographic projection apparatus, a pattern (e.g. in a mask) is imaged onto a substrate that is at least partially covered by a layer of radiation-sensitive material (resist). Prior to this imaging step, the substrate may undergo various procedures, such as priming, resist coating and a soft bake. After exposure, the substrate may be subjected to other procedures, such as a post-exposure bake (PEB), development, a hard bake and measurement/inspection of the imaged features. This array of procedures is used as a basis to pattern an individual layer of a device, e.g. an IC. Such a patterned layer may then undergo various processes such as etching, ion-implantation (doping), metallization, oxidation, chemo-mechanical polishing, etc., all intended to finish off an individual layer. If several layers are required, then the whole procedure, or a variant thereof, will have to be repeated for each new layer. Eventually, an array of devices will be present on the substrate (wafer). These devices are then separated from one another by a technique such as dicing or sawing, whence the individual devices can be mounted on a carrier, connected to pins, etc.. Further information regarding such processes can be obtained, for example, from the book "Microchip Fabrication: A Practical Guide to Semiconductor Processing", Third Edition, by Peter van Zant, McGraw Hill Publishing Co., 1997, ISBN 0-07-067250-4, incorporated herein by reference.

For the sake of simplicity, the projection system may hereinafter be referred to as the "lens"; however, this term should be broadly interpreted as encompassing various types of projection system, including refractive optics, reflective optics, and catadioptric systems, for example. The radiation system may also include components operating according to any of these design types for directing, shaping or controlling the projection beam of radiation, and such components may also be referred to below, collectively or singularly, as a "lens". Further, the lithographic apparatus may be of a type having two or more substrate tables (and/or two or more mask tables). In such "multiple stage" devices the additional tables may be used in parallel, or preparatory steps may be carried out on one or more tables while one or more other tables are being used for exposures. Dual stage lithographic apparatus are described, for example, in US 5,969,441 and WO 98/40791, incorporated herein by reference.

To enable imaging of smaller features than is possible with current lithographic projection apparatus, it is proposed to use extreme ultraviolet radiation (EUV), e.g. with a

wavelength of 13.5nm, as the exposure radiation. Such radiation is strongly absorbed by almost all known materials and so it is necessary to use a reflective mask. However, making a reflective mask for EUV presents its own problems and to achieve an acceptable reflectance, the mask must be formed as a distributed Bragg reflector formed by a multilayer of 40 or more layer pairs of, for example, (Mo/Si) or (Mo/Be). The mask pattern is then formed by an overlying patterned absorber layer such as Tantalum (Ta) or Chrome (Cr). The multilayer and absorber layer must be relatively thick, many tens of wavelengths, and this, coupled with the necessity to illuminate the mask obliquely, introduces various errors in the projected image, as compared to an ideal, thin binary mask.

These errors are discussed in various publications. B. S. Bollepalli and F. Cerrina, *On the Computation of Reflected Images from Extreme Ultra Violet Masks*, SPIE Conference on Emerging Lithographic Technologies III, Santa Clara, CA, SPIE Volume 3676, 587-597 (March 1999) describes variation of line widths and pattern shifts with angle of incidence of isolated structures and proposes correction by a suitable mask bias. C. G. Krautschik, M. Ito, I. Nishiyama, and K. Otaki, *Impact of the EUV mask phase response on the asymmetry of Bossung curves as predicted by rigorous EUV mask simulations,* SPIE Conference on Emerging Lithographic Technologies V, Santa Clara, CA, SPIE Volume 4343 (March 2001) describes asymmetry of the Bossung curve through focus for isolated structures and indicates that different illumination angles experienced by horizontal and vertical lines causes an additional horizontal to vertical CD bias through focus. Again, it is proposed to compensate for these effects through mask-sizing schemes. K Otaki, *Asymmetric properties of the Aerial Image in Extreme Ultraviolet Lithography*, Jpn. J. Appl. Phys. Vol 39 (2000) pp 6819-6826, describes the influence of asymmetric diffraction when a thick mask is asymmetrically illuminated and notes the asymmetry in the aerial image.

However, the solutions proposed in the prior art do not provide complete solutions and cannot compensate for all mask-induced effects.

It is an object of the present invention to provide a device manufacturing method using a reflective mask illuminated at an angle to the normal in which improved imaging is obtained.

This and other objects are achieved according to the invention in a device manufacturing method as specified in the opening paragraph, characterized in that:

system aberrations in the projection system used in said step of projecting the patterned beam are controlled or created to compensate for mask-induced aberrations.

In the method of the invention, it is possible to compensate for best focus shift effects due to a reflective mask and oblique illumination in such a way that best focus shift differences between dense and isolated lines, and between horizontal and vertical lines, can be reduced. The invention uses any available "knobs" in the projection system to effect wavefront or phase manipulation to correct any correctables in the image shape. This assists in bringing process windows for different features closer together. It is also possible to use iso-focal tilt as the metric for level of aberration input and reduce the differences between different structure types. The choice of metric is important as improvement in isofocal tilt may worsen best focus shift performance, and vice versa.

The method of the present invention can also compensate for mask-induced image CD offset, which occurs as a function of mask angle of incidence (MAI), absorber thickness, feature type and NA/illumination settings. The dominant effect is a CD variation between features as a function of structural orientation, for example a horizontal-vertical (HV) bias varying across the image field. For contact holes, the mask will induce ellipticity variation across the image field.

Preferably, the low order system aberrations are Z5 astigmatism, Z9 spherical, and Z12 astigmatism (as defined below) or equivalent aberrations. Simulations of dense and semi-isolated structures, with and without aberrations, have provided sensitivity data for best focus (BF) shift and isofocal tilt (IFT). Optimized combinations of Zernikes Z5, Z9 and Z12 can compensate for, and reduce, best focus shifts and isofocal tilt to bring focus positions of dense, semi-isolated, horizontal and vertical lines of same critical dimension (CD) closer together. Thus, the possibility of overlapping process windows for imaging is enhanced. The effect of using such best focus shift compensation can also have a positive effect on isofocal tilt but this is feature dependent. Contact hole ellipticity variation across the image field can be compensated for using mostly Z5 astigmatism. HV bias variation

can be compensated for in combination with best focus shift and iso-focal tilt using principally combinations of Z5, Z9 and Z12 aberrations.

A further problem that the invention may address is image displacement in the XY plane. Such displacements may occur as a function of mask angle of incidence, absorber thickness, feature type and NA/illumination settings and the displacements will be dependent on position in the image field. Whilst such effects may be compensated for in some cases by pre-distortion of the mask and by optical proximity corrections, these solutions tie the mask to use with a particular set of machine settings. A more flexible solution can be provided by the invention by controlling and/or introducing projection system aberrations, particularly Z2, Z3, and Z7 (as defined below).

A further aspect of the present invention provides a computer program for determining low order system aberrations to be effected in a projection system of a lithographic apparatus to optimize imaging of a reflective mask embodying a mask pattern, the program comprising code means that, when executed on a computer system, instruct the computer to perform the steps of:

determining the sensitivities of different features in said pattern to different aberrations;

determining the optimum combination of aberrations using the determined sensitivities.

Another aspect of the invention provides a computer program for controlling a lithographic projection apparatus to effect low order system aberrations in the projection system of the lithographic projection apparatus to optimize imaging of a reflective mask embodying a mask pattern.

Although specific reference may be made in this text to the use of the apparatus according to the invention in the manufacture of ICs, it should be explicitly understood that such an apparatus has many other possible applications. For example, it may be employed in the manufacture of integrated optical systems, guidance and detection patterns for magnetic domain memories, liquid-crystal display panels, thin-film magnetic heads, etc. The skilled artisan will appreciate that, in the context of such alternative applications, any use of the terms "reticle", "wafer" or "die" in this text should be considered as being replaced by the more general terms "mask", "substrate" and "target portion", respectively.

Embodiments of the invention will now be described, by way of example only, with reference to the accompanying schematic drawings in which:

Figure 1 depicts a lithographic projection apparatus that may be used to carry out the method of the invention;

Figure 2 depicts a reflective multilayer mask that may be used in the method of the invention;

Figure 3 is a flow diagram of a method according to the invention;

Figure 4 is a diagram of a system for applying corrections determined in the method of the invention;

Figure 5 is a graph of best focus shift vs. pitch for 30nm lines on a bright field without any correction according to the invention being applied;

Figure 6 is a graph of isofocal tilt vs. pitch for 30nm lines on a bright field without any correction according to the invention being applied;

Figures 7 to 11 are graphs showing the effects on best focus shift and isofocal tilt with various degrees of correction according to the method of the invention;

Figures 12 to 15 are graphs of critical dimension vs. focus for various illumination conditions and degrees of correction;

Figure 16 is a graph of critical dimension uniformity vs. added focus range for illumination conditions and degrees of correction;

Figure 17 is a graph of image critical dimension as a function of mask angle of incidence and pitch;

Figure 18 is a graph of mask-induced critical dimension and horizontal-vertical bias as a function of position in the image field; and

Figure 19 is a graph of image displacement as a function of mask angle of incidence and pitch.

In the Figures, corresponding reference symbols indicate corresponding parts.

Lithographic Projection Apparatus

Figure 1 schematically depicts a lithographic projection apparatus that may be used to perform the method of the invention. The apparatus comprises:

- a radiation system Ex, IL, for supplying a projection beam PB of radiation (*e.g.* EUV radiation), which in this particular case also comprises a radiation source LA;
- a first object table (mask table) MT provided with a mask holder for holding a mask MA (*e.g.* a reticle), and connected to first positioning means for accurately positioning the mask with respect to item PL;
- a second object table (substrate table) WT provided with a substrate holder for holding a substrate W (*e.g.* a resist-coated silicon wafer), and connected to second positioning means for accurately positioning the substrate with respect to item PL;
- a projection system ("lens") PL (*e.g.* mirror group) for imaging an irradiated portion of the mask MA onto a target portion C (*e.g.* comprising one or more dies) of the substrate W.

As here depicted, the apparatus is of a reflective type and has a reflective mask.

The source LA (*e.g.* a laser-produced or discharge plasma source) produces a beam of radiation. This beam is fed into an illumination system (illuminator) IL, either directly or after having traversed conditioning means, such as a beam expander Ex, for example. The illuminator IL may comprise adjusting means AM for setting the outer and/or inner radial extent (commonly referred to as σ-outer and σ-inner, respectively) of the intensity distribution in the beam. In addition, it will generally comprise various other components, such as an integrator IN and a condenser CO. In this way, the beam PB impinging on the mask MA has a desired uniformity and intensity distribution in its cross-section.

It should be noted with regard to Figure 1 that the source LA may be within the housing of the lithographic projection apparatus (as is often the case when the source LA is a mercury lamp, for example), but that it may also be remote from the lithographic projection apparatus, the radiation beam which it produces being led into the apparatus (e.g. with the aid of suitable directing mirrors); this latter scenario is often the case when the source LA is an excimer laser. The current invention and Claims encompass both of these scenarios.

The beam PB subsequently intercepts the mask MA, which is held on a mask table MT. Having been selectively reflected by the mask MA, the beam PB passes through the lens PL, which focuses the beam PB onto a target portion C of the substrate W. With the aid of the second positioning means (and interferometric measuring means IF), the substrate table WT can be moved accurately, *e.g.* so as to position different target portions C in the path of the beam PB. Similarly, the first positioning means can be used to accurately position the mask MA with respect to the path of the beam PB, *e.g.* after mechanical retrieval of the mask MA from a mask library, or during a scan. In general, movement of the object tables MT, WT will be realized with the aid of a long-stroke module (course positioning) and a short-stroke module (fine positioning), which are not explicitly depicted in Figure 1. However, in the case of a wafer stepper (as opposed to a step-and-scan apparatus) the mask table MT may just be connected to a short stroke actuator, or may be fixed.

The depicted apparatus can be used in two different modes:

1. In step mode, the mask table MT is kept essentially stationary, and an entire mask image is projected in one go (*i.e.* a single "flash") onto a target portion C. The substrate table WT is then shifted in the x and/or y directions so that a different target portion C can be irradiated by the beam PB;

2. In scan mode, essentially the same scenario applies, except that a given target portion C is not exposed in a single "flash". Instead, the mask table MT is movable in a given direction (the so-called "scan direction", *e.g.* the y direction) with a speed v, so that the projection beam PB is caused to scan over a mask image; concurrently, the substrate table WT is simultaneously moved in the same or opposite direction at a speed $V = Mv$, in which M is the magnification of the lens PL (typically, $M = 1/4$ or $1/5$). In this manner, a relatively large target portion C can be exposed, without having to compromise on resolution.

Figure 2 shows the mask MA, which comprises a substrate 1 on which is provided a multilayer 2 forming a distributed Bragg reflector overlain by a patterned absorber layer 3. The multilayer may comprise 40 or more periods of alternating layers of Molybdenum (Mo) and Silicon (Si) or Molybdenum and Beryllium (Be). Other materials and three or four layer periods may also be used. Further details of suitable reflectors formed of multilayer stacks may be found in EP-A-1 065 532, EP-A-1 065 568 and European Patent

Application no 02253475.4. Each period of the multilayer is approximately half a wavelength thick so that the total thickness of the multilayer, T_{ml}, is about 270nm or more. Absorber layer 3 may be formed of Tantalum (Ta) or Chrome (Cr) and to provide a sufficient degree of absorption, its thickness, T_a, is 50 or 100nm or more.

Because the illumination and projection systems are formed of reflective optical elements, the mask must be illuminated obliquely, e.g. at an angle, θ_i, of about 6° to the normal.

The combination of the oblique illumination and the thickness of the multilayer and absorber layer causes a number of deformations in the projected image, as compared to the image that would be produced by an ideal, thin binary mask. As can easily be seen, the shadowing effect of the thick absorber will cause opaque features to be imaged with greater width than the feature on the mask and this effect will differ between horizontal and vertical features because of the different effective angle of illumination. The thickness of the multilayer and the extent to which the illumination radiation penetrates the multilayer further complicates the situation and introduces various phase effects.

The various effects of the thick, reflective mask can be simulated and are found to be pattern dependent - the effects on vertical and horizontal lines differ and the effects are different according to pattern density for example. The resulting deformations of the aerial images may be characterized as or approximated by aberrations, which can be expressed in terms of Zernike polynomials. According to the invention, aberrations in the projection system are introduced and/or controlled to counteract the effects of the mask thickness and oblique illumination.

The aberrations may be introduced or controlled by control of the position and/or orientations of the individual mirrors of the projection system and the mask and substrates. Positioning systems for the individual mirrors of the projection system are included in an EUV lithographic projection system to provide the necessary image stability and may be used to effect the aberration control of the present invention without further modification, simply by the use of different setpoints. The present invention may, alternatively or in addition, make use of adaptive mirrors, such as described in EP-A-1 174 770.

Figure 3 illustrates a basic process of the invention. For a specific mask pattern, first the image deformations that will occur in imaging it are calculated in step S1. Next, the required corrective aberrations are calculated in step S2 and the table position and

mirror position and/or shape changes required to effect these aberrations are calculated in step S3. The calculated changes are applied to the projection system in step S4 before imaging takes place in step S5. Steps S1 to S3 may be carried out in advance of a projection and the results transferred to the lithographic projection system when required. If the image deformations vary across the pattern to be imaged and the relevant actuators are sufficiently responsive, the relevant changes may be applied during an imaging scan as well as in advance of it.

A system to effect the method of the invention is shown in Figure 4. The mask pattern data or precomputed settings for the stage and mirror positions and/or shapes are provided to the central control system CCS of the lithographic apparatus. If mask pattern data are provided, the central control system computes the desired settings for the stage and mirror positions and/or shapes. Prior to and/or during a scanned exposure, the central control system controls the mask table MT and substrate table WT positions, via respective positioning system PM, PW, as well as the positions and/or shapes of some or all mirrors M1, M2 in the projection system PL, via respective control system MCS1, MCS2. Only two mirrors in the projection system PL are shown in Figure 4 however, the projection system may comprise four or more mirrors.

In a preferred embodiment of the invention, the aberrations introduced to control the mask-induced effects are defined by Zernike polynomials Z5 (astigmatism HV), Z9 (spherical aberration) and Z12 (astigmatism HV – higher order). Other aberrations that might be used include Z2 (tilt in X), Z3 (tilt in Y), Z4 (defocus), Z6 (astigmatism 45°/135°), Z7 (coma X), Z8 (coma Y) and Z13 (astigmatism 45°/135° - higher order). These polynomials take the form:

Z2: $r \cdot \cos(\theta)$

Z3: $r \cdot \sin(\theta)$

Z4: $2 \cdot r^2 - 1$

Z5: $r^2 \cdot \cos(2 \cdot \theta)$

Z6: $r^2 \cdot \sin(2 \cdot \theta)$

Z7: $(3 \cdot r^3 - 2 \cdot r) \cdot \cos(\theta)$

Z8: $(3 \cdot r^3 - 2 \cdot r) \cdot \sin(\theta)$

Z9: $6 \cdot r^4 - 6 \cdot r^2 + 1$

Z12: $\left(4 \cdot r^4 - 3 \cdot r^2\right) \cdot \cos(2 \cdot \theta)$

Z13: $\left(4 \cdot r^4 - 3 \cdot r^2\right) \cdot \sin(2 \cdot \theta)$

Z4 can be used to correct a focus shift independent of structure size and type. Z6 and Z13 have the same effect on the difference between 45° and 135° degree lines as do Z5 and Z12 on the difference between horizontal and vertical lines. Z5 and Z6 are equally important in correcting contact hole ellipticity. Z7 and Z8 affect horizontal and vertical lines respectively.

Higher order aberrations may also be employed to improve control if desired and/or feasible.

It is noted that Zernike polynomials may be expressed in different forms, for example with and without normalization coefficients, and may be numbered in various sequences, e.g. increasing in order of angle then radius or *vice versa*. Also, other forms for the expression of aberrations are known, e.g. Seidel aberration polynomials. The present invention is not limited to a particular form of expression of the aberrations introduced and embraces the calculation of and addition of aberrations expressed in other forms.

Example 1

An example of the invention, which has been simulated, will now be described.

Images without aberration - pure - were simulated for both horizontal and vertical lines at dense and semi isolated for 30nm and 50nm features. Due to the simulator software, horizontal lines had to be simulated as vertical, but corrections in aberration sensitivity have been made for this. Best Focus shifts and Isofocal Tilt were calculated.

More simulations were then performed for the same features with 1nm of a single aberration input. Analysis of Best Focus shifts and Isofocal Tilts were repeated. Sensitivity data was calculated for each feature and aberration combination. Sensitivity is equal to the change in a parameter due to (+)1nm of an aberration. (For best focus shift the sensitivity units are nm/nmaberration and for isofocal tilt, nm/μmfocus/nmaberration). Only Prolith™ relative sensitivities for aberrations are considered here for optimization purposes i.e. changes in best focus shift or isofocal tilt relative to the position of the "pure"

image. These results best describe the baseline before aberration input and are often the standard technique for assessing process windows. Note that the positive and negative shift positions, and associated sensitivities, are described here in terms of the system coordinates.

The present invention aims to position the focus shifts and isofocal tilt values to remove the differences between horizontal and vertical features, and between dense and isolated features, thus allowing overlap of the process windows and enabling a wider range of simultaneous imaging. Ideally, all features, of different shapes, linewidths, pitches (whether isolated or dense) and orientations should have a common best focal plane, i.e. all best focus shift values are the same, and an iso-focal tilt of zero. Each Zernike aberration works on different feature types and orientations in a different way. By programming an Excel™ sheet to automatically plot the resultant position after interaction with a single Zernike or several Zernikes, it is possible to experiment with different combinations and levels of Zernike input, to flatten out the plots (removing pitch dependence) and to bring the H and V plots closer together. Zernikes can be input in either the positive or negative directions in the system.

As an example of the method employed, 30nm lines on a bright field mask were considered. The initial best focus shift and isofocal tilt results for pure images for normal incidence, equivalent to system vertical lines, and 6° incidence, equivalent to system horizontal lines, are shown below for different pitches. Also detailed are the calculated sensitivity values with respect to Z5 and Z12 astigmatism and Z9 spherical for normal and 6° incidence. These Zernikes can be adjusted in a lithographic projection apparatus.

Table 1 BFshifts and IFT : pure images, starting values

	BFshift_V	BFshift_H	IFT_V	IFT_H
pitch 60nm (D)	-5	10	-0.5	-0.5
pitch 150nm (I)	5	20	8	8.5

Table 2: Relative Sensitivities (in system co-ordinates)

Fshift	dense		iso		IFT	dense		iso	
	N	6	N	6		N	6	N	6
Z5	-25	40	-25	40	Z5	0	0.5	-0.5	0
Z12	-5	20	15	-25	Z12	-1.5	1.5	6	-5.5
Z9	20	5	55	60	Z9	-1.5	-1.5	11	6.5

When plotted, the starting positions for BFshift and IFT appear as shown in Figures 5 and 6. The differences in parameters between dense and isolated lines and between horizontal and vertical lines are clearly visible.

The best results so far for 30nm and 50nm bright field lines are shown in Figures 7 to 17, together with the effect on IFT, which such a correction would trigger. Note that from the starting position Zernikes are added in the order of the graph legend, thus the last Zernike in the list is the final position of the BF and IFT plots and a summation of all Zernike inputs.

Figure 7 shows the effect of adding aberrations to correct for best focus shift due to the mask. The values of the Zernike aberrations added were: Z5= -0.26nm, Z9=-0.24nm and Z12=-0.07nm. Figure 8 then illustrates the effect of the correction on isofocal tilt. A clear improvement can be seen - both the best focus shift and isofocal tilt become less dependent on pitch after the corrective aberrations are introduced.

The best results obtained for different features are shown in Table 3 below:

	Z5 (nm)	Z9 (nm)	Z12 (nm)	starting focus range (nm)	resulting focus range (nm)	starting IFT maxvalue	IFT max after BF correction
30nm	-0.26	-0.24	-0.07	25	0	8.5	7.3
50nm	-0.18	-0.22	-0.18	15	0	10.5	7.8

Comparing Figures 7 and 9, illustrates the improvements obtained for 30nm and 50nm lines in a bright field.

Of course it is also possible to optimize for IFT. However, this results in a different set of aberration inputs and thus affects the BFshift positions. Examples for 30nm and 50nm lines on bright field mask are shown in Table 4 below:

	Z5 (nm)	Z9 (nm)	Z12 (nm)	starting focus range (nm)	resulting focus range (nm)	starting IFT maxvalue	IFT max after BF correction
30nm	-0.4	-0.55	0.11	25	25	8.5	4.3
50nm	-0.34	-0.37	-0.11	15	15	10.5	6.1

These results are shown in Figures 10, for 30nm lines, and 12, for 50nm lines.

It is further possible to search for a combination of aberrations that give the best solution for both best focus shift and isofocal tilt, which involves weighting the relative importance of best focus shift and isofocal tilt.

The above examples demonstrate that it is possible to compensate for BFshift effects due to a reflective mask and oblique illumination in such a way that BFshift differences between dense and isolated lines, and between horizontal and vertical lines, can be reduced. This will assist in bringing process windows for different features closer together. It is also possible to use IFT as the metric for level of aberration input and reduce the differences between different structure types. The choice of metric is important as improvement in IFT may worsen BFshift performance, and visa versa.

To confirm the usefulness of the invention, using the adjustments described above, images in resist were simulated to investigate the effect of correction of BFshifts on CDU (Critical Dimension Uniformity). Prolith™ was used for simulation with the EUV-2D resist model, resist thickness 120nm. A CDU prediction model used the resist images as a base and, together with user inputs of focus and energy budgets, calculated the resultant CDU performance for various focus ranges. Figures 12 to 16 clearly show that altering the IFT and BF parameters enhances the CDU performance, thus indicating the relevance of BFshift and IFT correction by aberration input.

Figure 12 shows the simulated CD response in resist versus energy and focus for 30nm isolated lines printed with NA=0.25, σ=0.5 and 6 degrees MAI, thus representing the horizontal lines. In the graph, the three elliptically shaped CD contours indicate the CD variation as function of system energy and focus errors. Each CD contour has represents a different focus setting, 0 and +/-100nm. The CD response in Figure 12 shows a mask-induced isofocal tilt leading to poor CD uniformity.

Figure 13 shows the CD response versus energy and focus that is mathematically corrected for the isofocal tilt. The three CD contours show less CD variation indicating

that this tilt correction improves CD uniformity. Figure 14 shows the CD response in resist for 0 degrees MAI presenting the vertical lines. Figure 15 shows that again isofocal tilt correction improves CDU.

Figure 16 combines all CDU information of Figures 12-15. The predicted CDU is plotted against the focus range. The impact of the mathematical best focus (BF) and isofocal tilt (IFT) correction on CDU are shown. For example, the CDU for 0nm focus range is based on the black CD contours where the best focus is set at 0nm. The CDU for 200nm focus range is based no all three CD contours for the 0 and +/-100nm focus settings.

The Figure shows that the CDU can be improved substantially by BF and IFT correction for both horizontal and vertical lines. The CDU improves most for the largest focus range.

Example 2

As a follow up to the first example, which addressed mask-induced focus related effects and solutions (Z plane), a second example addressed the mask-induced image CD and displacement effects and methods to compensate these (X-Y plane). The simulations results described here are based on the same Solid-EUV™ produced aerial images as in the first example. These aerial images were imported into Prolith™ v7.1 to calculate the image CD and displacement.

As function of mask angle of incidence (MAI), absorber thickness, feature type and NA/illumination setting a mask induced image CD offset will occur. The dominant effect is a CD variation between features as function of structural orientation such as a HV bias. For contact holes, the mask will induce ellipticity.

Figure 17 shows image CD as function of MAI and pitch for 30nm lines with NA=0.25, σ=0.5. It can be seen that the CD bias between MAI of 0 and 6 degrees is 2.9nm for dense lines and 2.8nm for (semi)isolated lines. This information yields a sensitivity of 0.5nm CD / degree MAI.

Figure 18 shows mask-induced CD and HV bias as function of slit position, based on the MAI variation for horizontal and vertical lines and the CD sensitivity to MAI. The issues are the HV bias, the HV bias and average CD variation across the slit.

The consequent mask-induced contact hole ellipticity variation across the slit may be compensated by projection lens aberrations, most notably astigmatism (Z5). The HV

bias can be compensated in combination with the BF and IFT compensation by optimized project lens aberration settings, most notably Z5, Z9 and Z12.

As function of mask angle of incidence (MAI), absorber thickness, feature type and NA/illumination setting a mask induced image displacement will occur. As with the image CD effects, the image displacement induced by the mask will be slit position dependent. Figure 19 shows image displacement as function of MAI and pitch for 30nm lines with NA=0.25, σ=0.5, demonstrating a strong bias between horizontal features, for which the mask angle of incidence is 6°, and vertical features for which the mask angle of incidence is 0°. This effect can be compensated for by the introduction of aberrations Z2, Z3 and Z7, where:

$$Z2 = r\cos\theta$$

$$Z3 = r\sin\theta$$

$$Z7 = (3r^3-2r)\cos\theta$$

Whilst specific embodiments of the invention have been described above, it will be appreciated that the invention may be practiced otherwise than as described. The description is not intended to limit the invention.

CLAIMS:

1. A device manufacturing method comprising the steps of:
- providing a substrate that is at least partially covered by a layer of radiation-sensitive material;
- providing a projection beam of radiation using a radiation system;
- using patterning means to endow the projection beam with a pattern in its cross-section;
- projecting the patterned beam of radiation onto a target portion of the layer of radiation-sensitive material,

characterized in that:

system aberrations in the projection system used in said step of projecting the patterned beam are controlled or created to compensate for mask-induced aberrations.

2. A method according to claim 1 wherein said aberrations are introduced and/or controlled so that values of at least one imaging metric for different feature types appearing in said pattern are brought closer together.

3. A method according to claim 2 wherein said at least one imaging metric is selected from the group comprising: best focus shift, isofocal tilt, critical dimension, critical dimension uniformity, overlay, pattern asymmetry, pitch linearity and iso-dense bias.

4. A method according to claim 2 or 3 wherein said different features have different densities, different orientations and/or different critical dimensions.

5. A method according to claim 2, 3 or 4 wherein said aberrations are introduced so as to bring process windows for said different features closer together.

6. A method according to any one of the preceding claims wherein said system aberrations comprise one or more of Zernike polynomials Z2 (tilt in X), Z3 (tilt in

Y), Z4 (defocus), Z5 (astigmatism HV), Z6 (astigmatism 45°/135°), Z7 (coma X), Z8 (coma Y), Z9 (spherical aberration), Z12 (astigmatism HV – higher order) and Z13 (astigmatism 45°/135° - higher order), where these polynomials take the form:

Z2: $r \cdot \cos(\theta)$

Z3: $r \cdot \sin(\theta)$

Z4: $2 \cdot r^2 - 1$

Z5: $r^2 \cdot \cos(2 \cdot \theta)$

Z6: $r^2 \cdot \sin(2 \cdot \theta)$

Z7: $\left(3 \cdot r^3 - 2 \cdot r\right) \cdot \cos(\theta)$

Z8: $\left(3 \cdot r^3 - 2 \cdot r\right) \cdot \sin(\theta)$

Z9: $6 \cdot r^4 - 6 \cdot r^2 + 1$

Z12: $\left(4 \cdot r^4 - 3 \cdot r^2\right) \cdot \cos(2 \cdot \theta)$

Z13: $\left(4 \cdot r^4 - 3 \cdot r^2\right) \cdot \sin(2 \cdot \theta)$

7. A method according to any one of the preceding claims wherein said aberrations are introduced and/or controlled by controlling the position, orientation and/or surface figure of at least one optical element in said projection system.

8. A method according to any one of the preceding claims further comprising the step of calculating for said pattern the optimum aberrations to be effected in said projection system

9. A method according to claim 8 wherein said step of calculating comprises the steps of:

determining the sensitivities of different features in said pattern to different aberrations;

determining the optimum combination of aberrations using the determined sensitivities.

10. A method according to claim 9 wherein said sensitivities are determined by simulating images of said different features with different amounts and/or combinations of aberrations.

11. A method according to claim 8, 9 or 10 wherein in said step of calculating, account is taken of one or more parameters to be used in said step of projecting, said parameters including mask angle of incidence (MAI), absorber thickness, feature type and NA/illumination settings.

12. A computer program for determining system aberrations to be effected in a projection system of a lithographic apparatus to optimize imaging of a reflective mask embodying a mask pattern, the program comprising code means that, when executed on a computer system, instruct the computer to perform the steps of:

determining the sensitivities of different features in said pattern to different aberrations;

determining the optimum combination of aberrations using the determined sensitivities.

13. A computer program according to claim 12 wherein said code means comprises code means for simulating images of said different features with different amounts and/or combinations of aberrations to effect said step of determining the sensitivities

14. A computer program according to claim 12 or 13 wherein said code means is adapted to determine optimum aberrations to be effected so that values of at least one imaging metric for different feature types appearing in said pattern are brought closer together.

15. A computer program according to claim 14 wherein said at least one imaging metric is selected from the group comprising: best focus shift, isofocal tilt, critical dimension, critical dimension uniformity, overlay, pattern asymmetry, pitch linearity and iso-dense bias.

16. A computer program according to claim 14 or 15 wherein said different features are dense and isolated lines, and/or horizontal and vertical lines, and/or lines of different widths.

17. A computer program according to claim 14, 15 or 16 wherein said code means is adapted to determine optimum aberrations to be effected so as to bring process windows for said different features closer together.

17. A computer program for controlling a lithographic projection apparatus to effect system aberrations in the projection system of the lithographic projection apparatus to optimize imaging of a reflective mask embodying a mask pattern.

18. A computer program according to any one of claims 11 to 17 wherein said system aberrations are Z5 astigmatism, Z9 spherical, and Z12 astigmatism.

ABSTRACT

Device Manufacturing Method and Computer Programs

System aberrations are effected in a projection system of a lithographic apparatus to optimize imaging of a thick reflective mask that is obliquely illuminated. The aberrations may include Z5 astigmatism, Z9 spherical, and Z12 astigmatism.

Fig. 3

Fig. 1

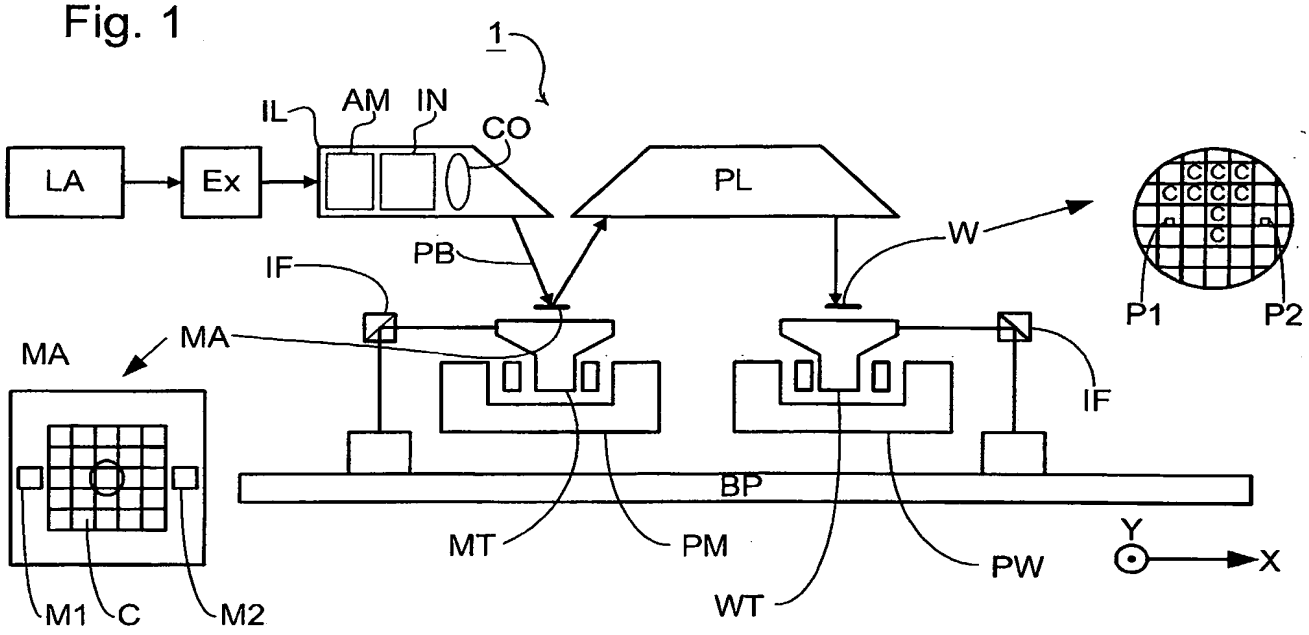

Fig. 2

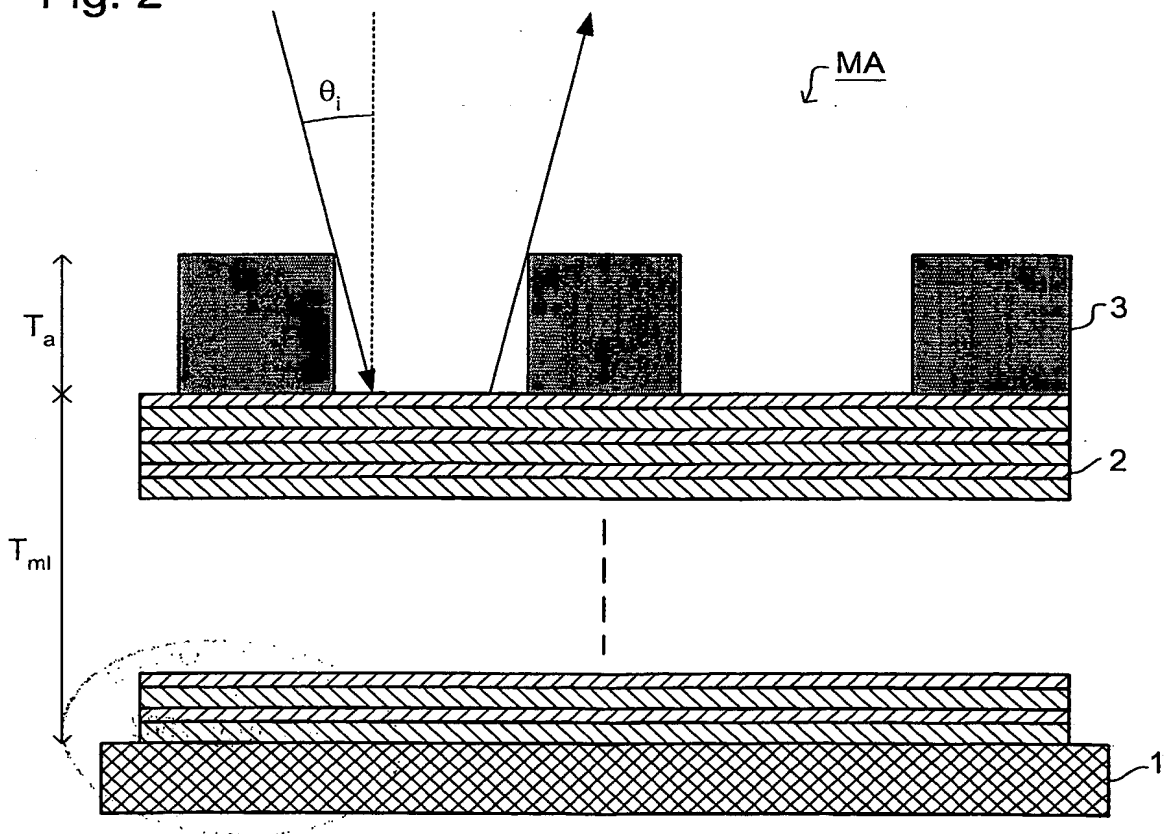

P-0393

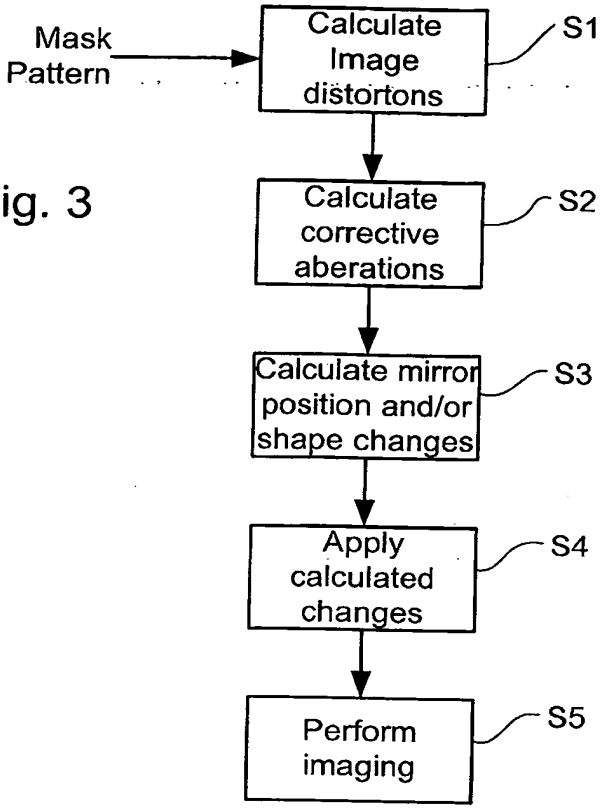

Fig. 3

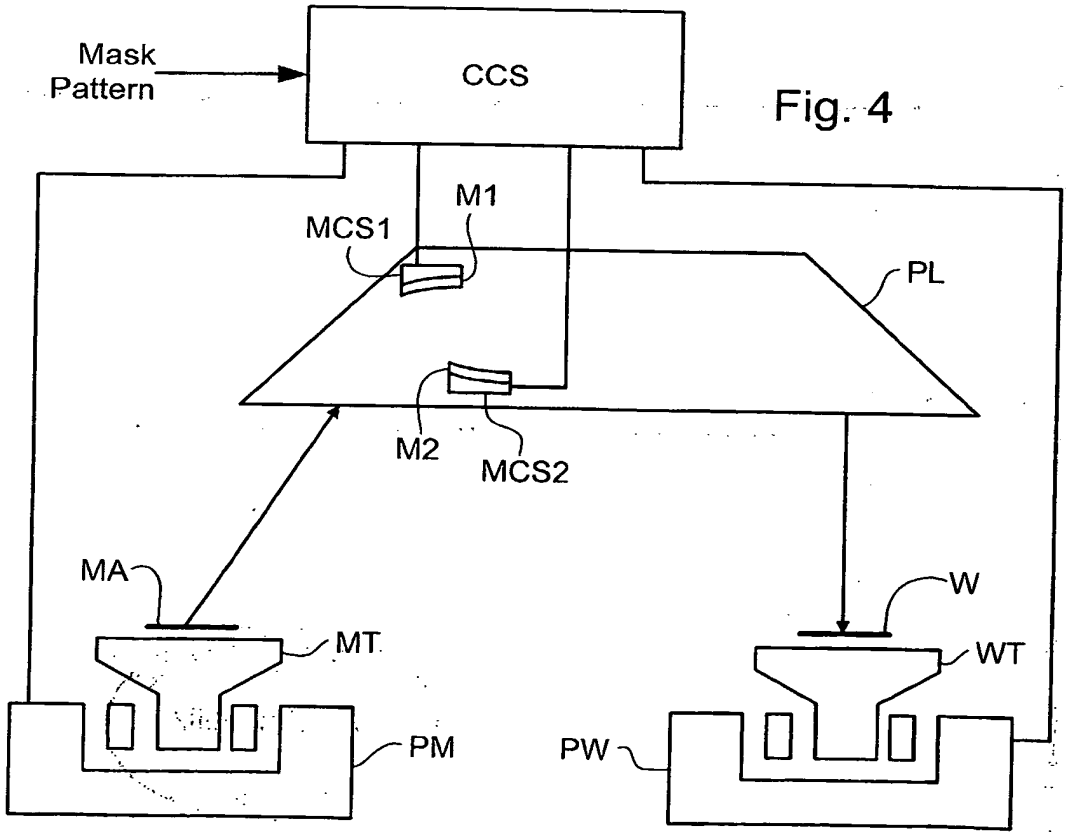

Fig. 4

P-0393

Fig. 5

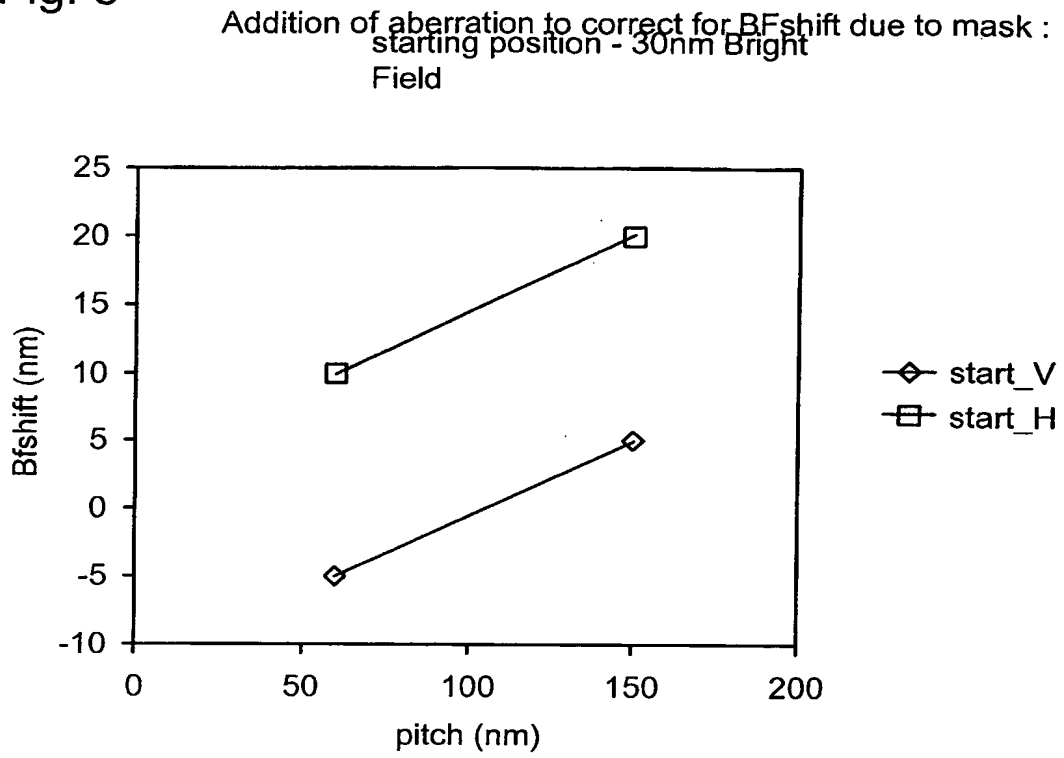

Fig. 6

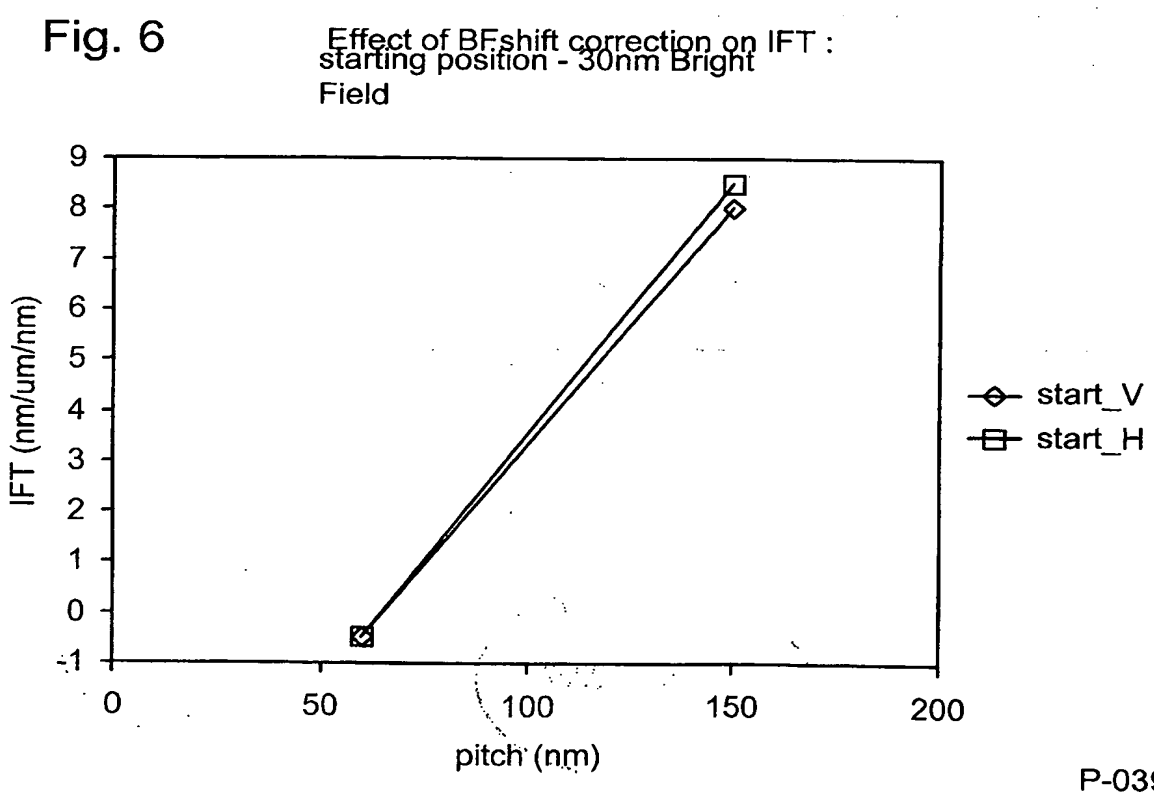

P-0393

Fig. 7

Addition of aberration to correct for BFshift due to mask :
Z5-0.26nm and Z9-0.24nm and Z12-0.07nm -30nm Bright Field

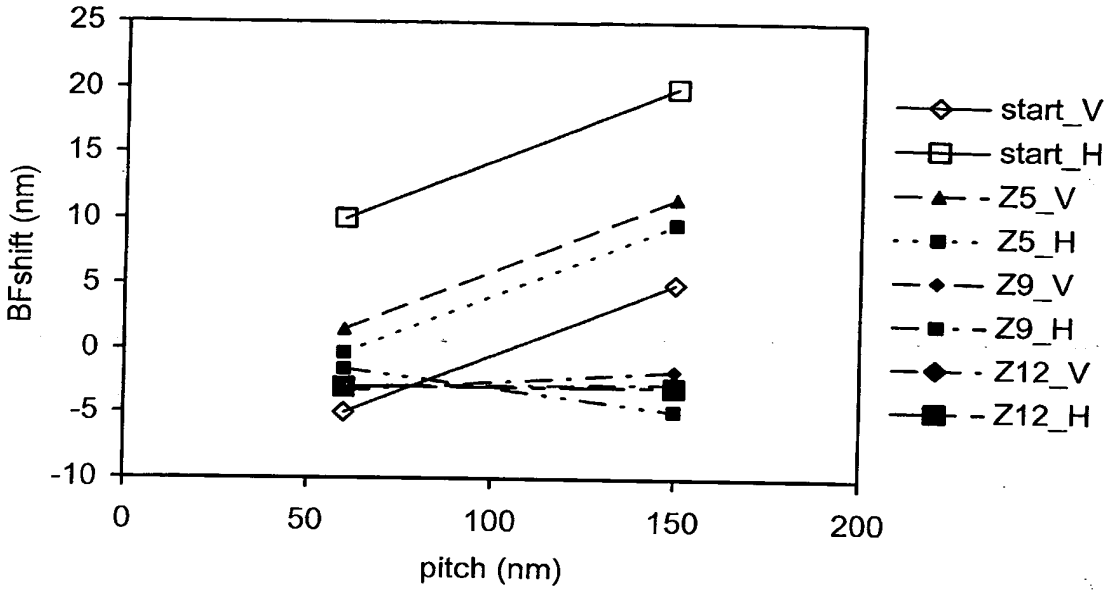

Fig. 8

Effect of BFshift correction on IFT :
Z5-0.26nm and Z9-0.24nm and Z12-0.07nm - 30nm Bright Field

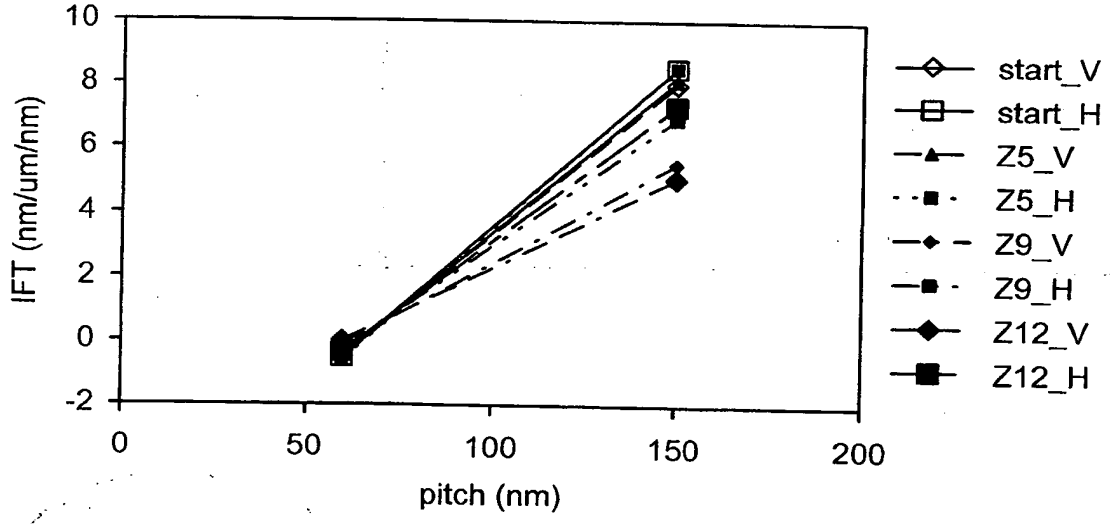

Fig. 9

Addition of aberration to correct for BFshift due to mask :
Z5-0.18nm and Z9-0.22 and Z12-0.18nm - 50nm Bright Field

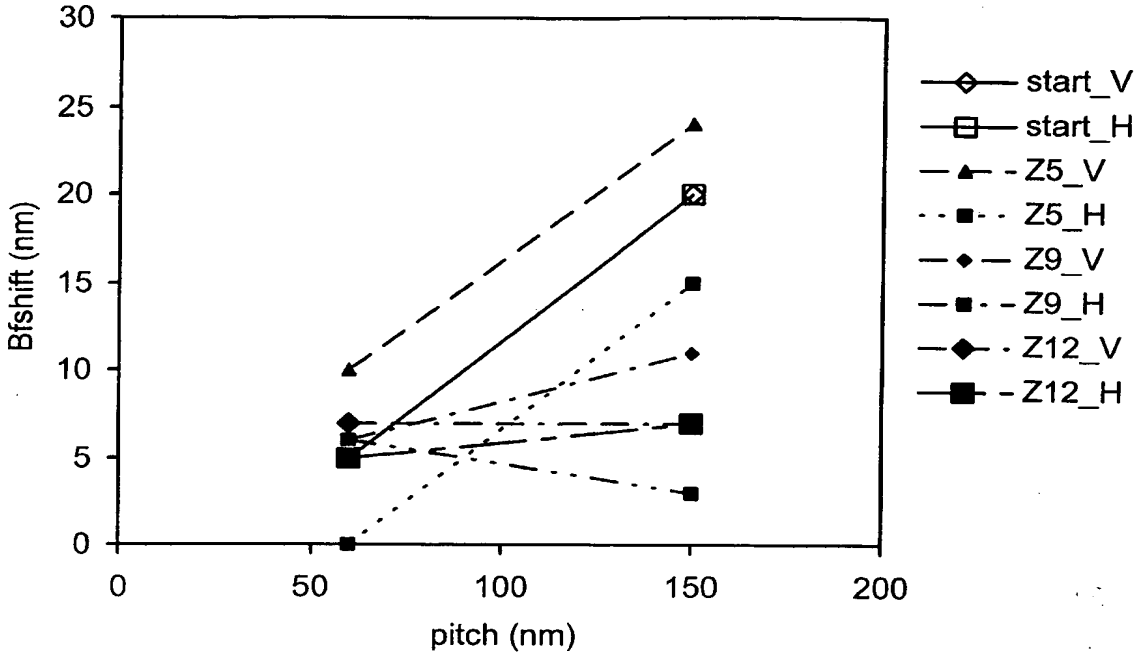

Fig. 10

Correction of IFT without impact on BFshifts :
Z5-0.4nm and Z9-0.55nm and Z12-0.11nm - 30nm Bright Field

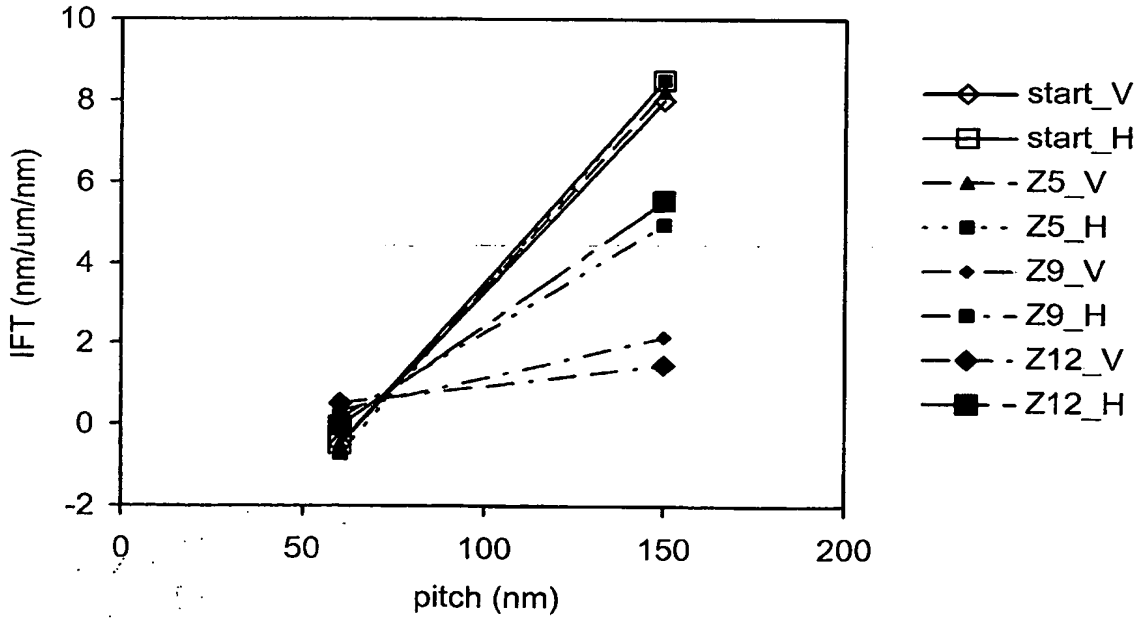

Fig. 11

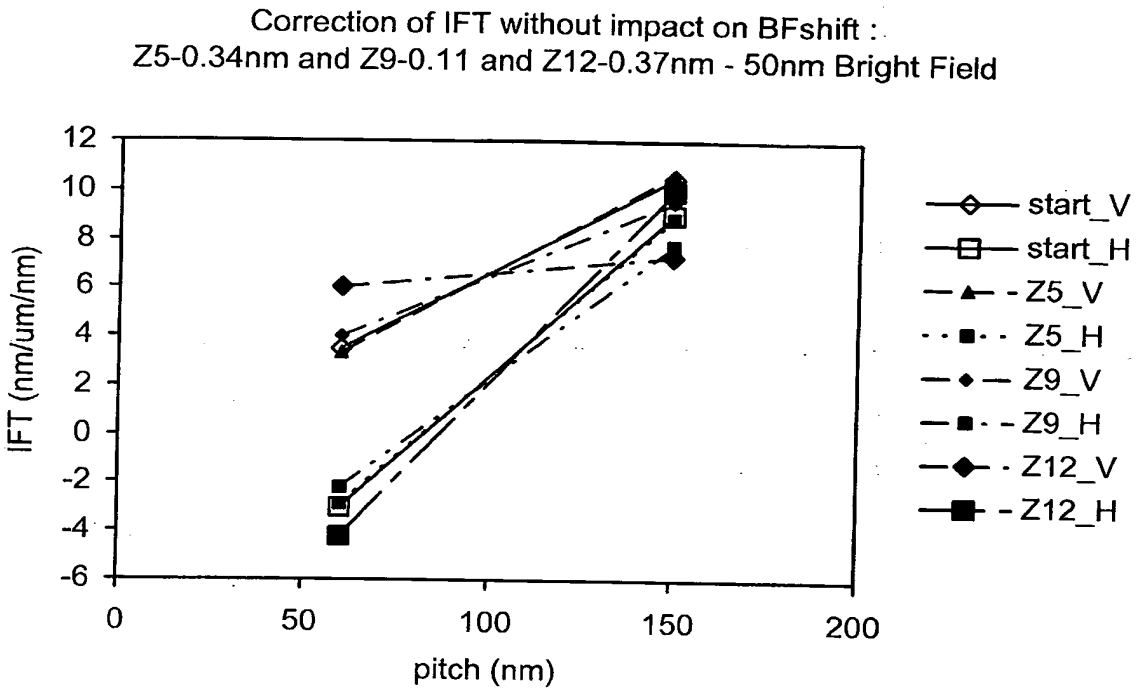

Fig. 12

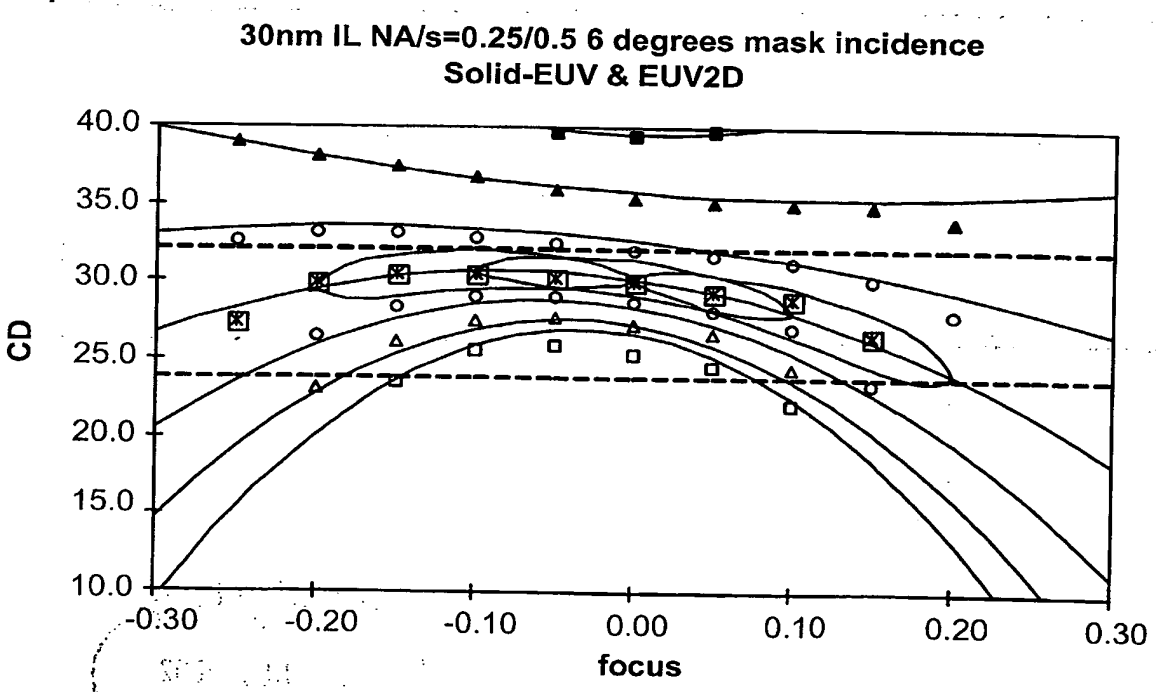

P-0393

Fig. 13

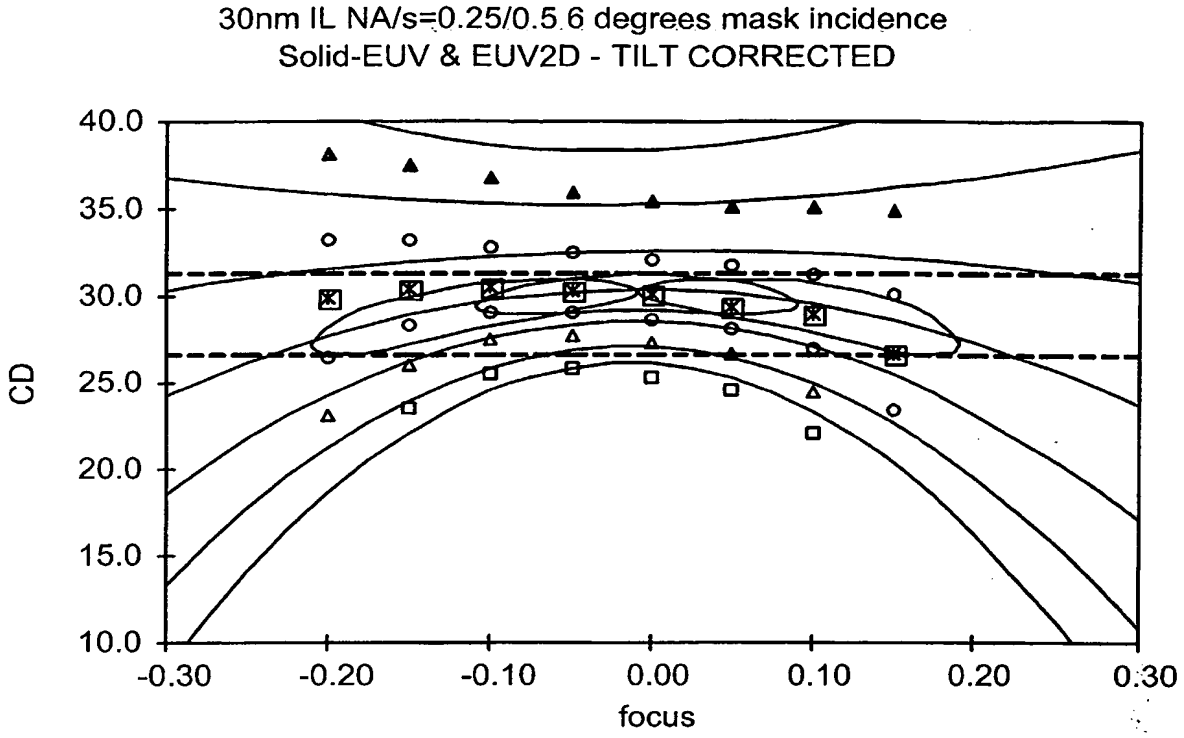
30nm IL NA/s=0.25/0.5 6 degrees mask incidence
Solid-EUV & EUV2D - TILT CORRECTED
CD
40.0
35.0
30.0
25.0
20.0
15.0
10.0
-0.30
-0.20
-0.10
0.00
0.10
0.20
0.30
focus

Fig. 14

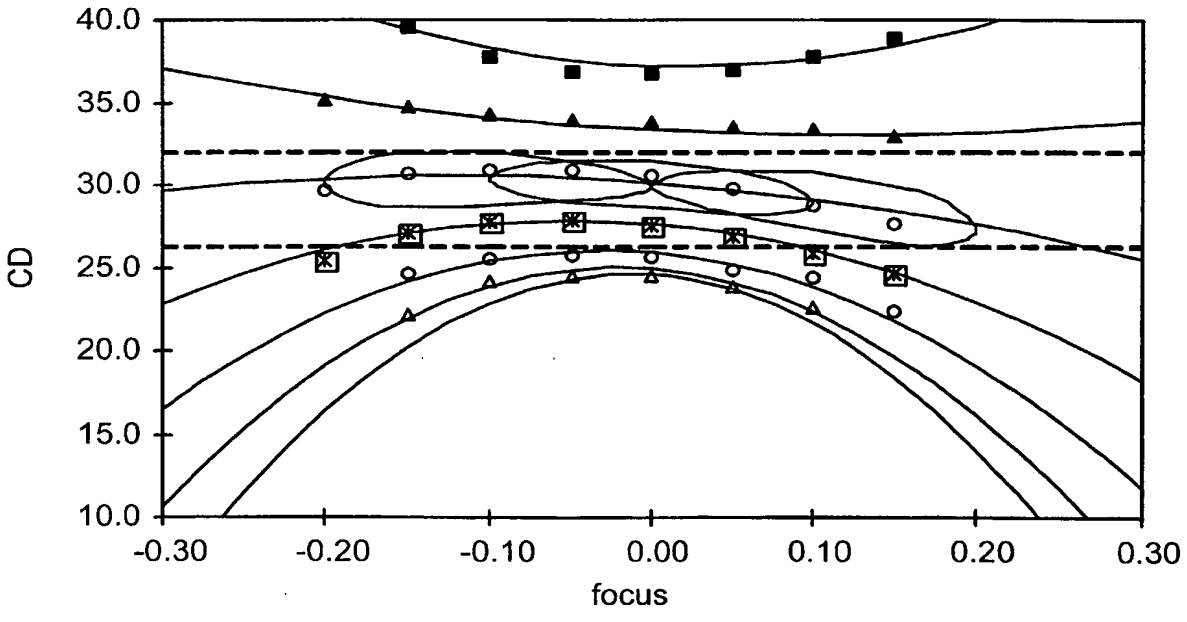
30nm IL NA/s=0.25/0.5 0 degrees mask incidence
Solid-EUV & EUV2D
CD
40.0
35.0
30.0
25.0
20.0
15.0
10.0
-0.30
-0.20
-0.10
0.00
0.10
0.20
0.30
focus

Fig. 15

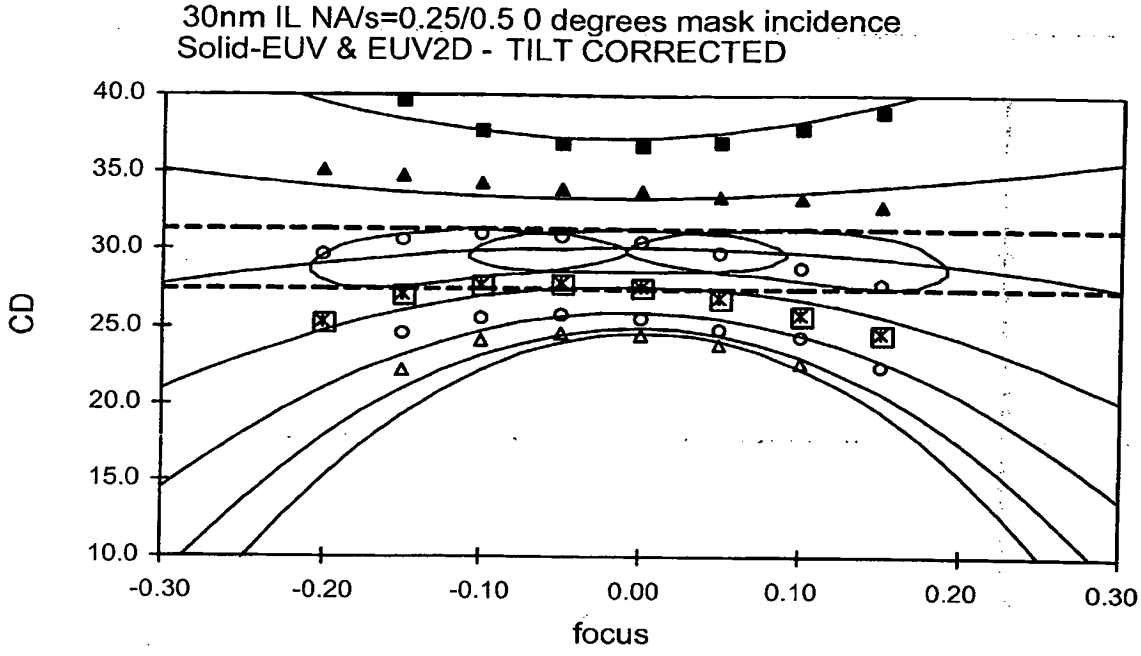
30nm IL NA/s=0.25/0.5 0 degrees mask incidence
Solid-EUV & EUV2D - TILT CORRECTED
CD
40.0
35.0
30.0
25.0
20.0
15.0
10.0
-0.30
-0.20
-0.10
0.00
0.10
0.20
0.30
focus

Fig. 16

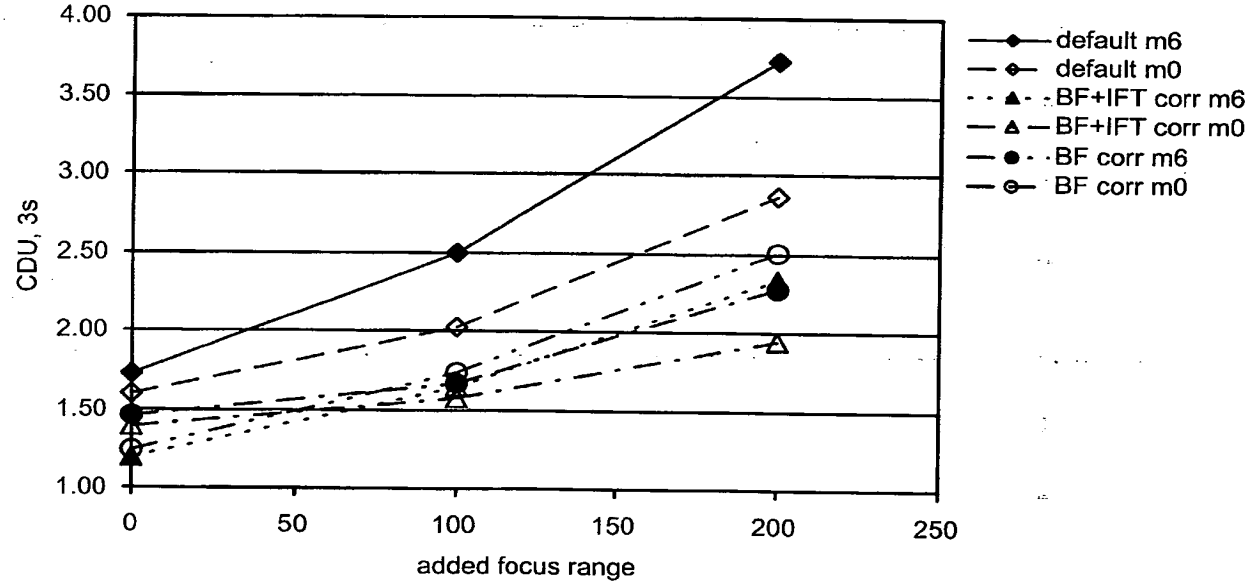
CDU, 3s
4.00
3.50
3.00
2.50
2.00
1.50
1.00
0
50
100
150
200
250
added focus range
default m6
default m0
BF+IFT corr m6
BF+IFT corr m0
BF corr m6
BF corr m0

Fig. 17

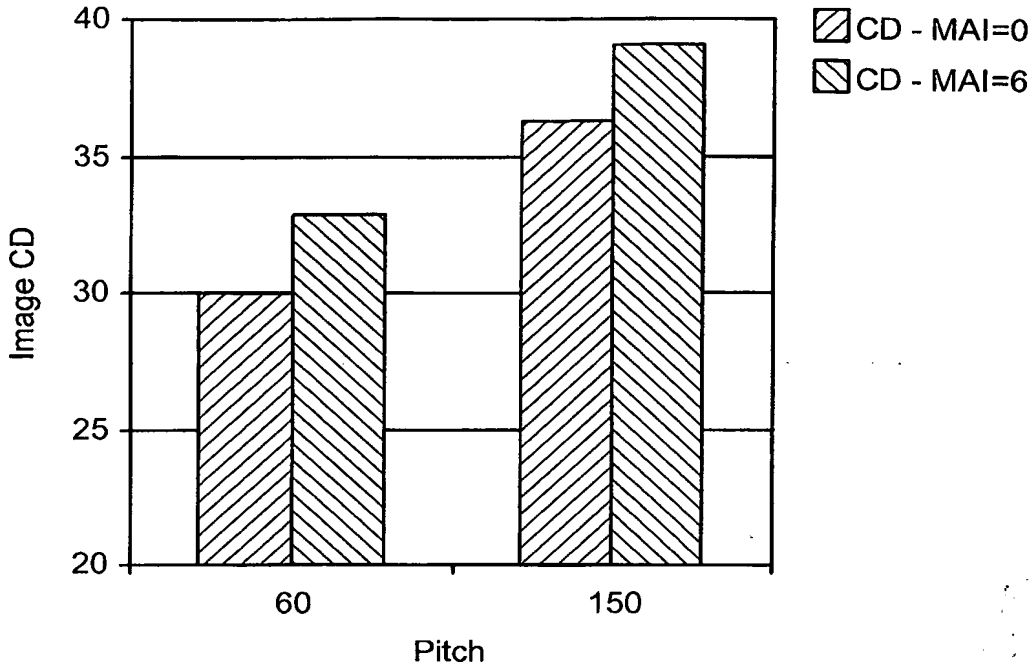
40
35
30
25
20
Image CD
60
150
Pitch
CD - MAI=0
CD - MAI=6

Fig. 18

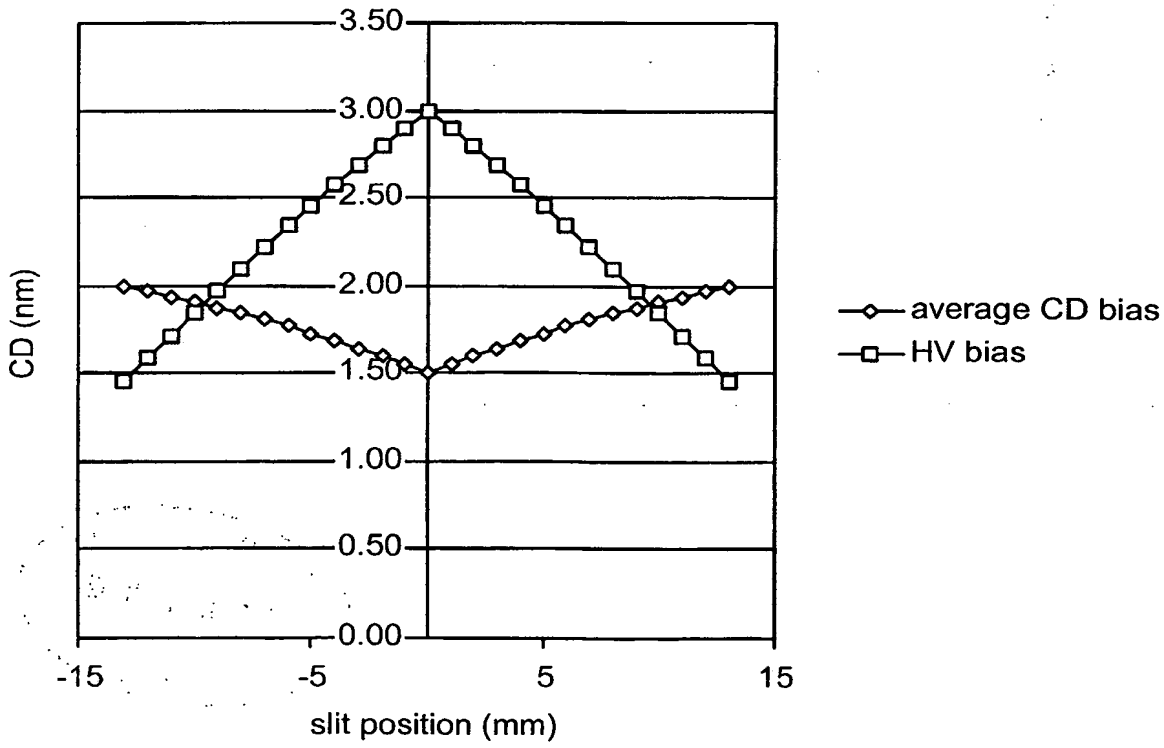
3.50
3.00
2.50
2.00
1.50
1.00
0.50
0.00
CD (nm)
-15
-5
5
15
slit position (mm)
average CD bias
HV bias

Fig. 19

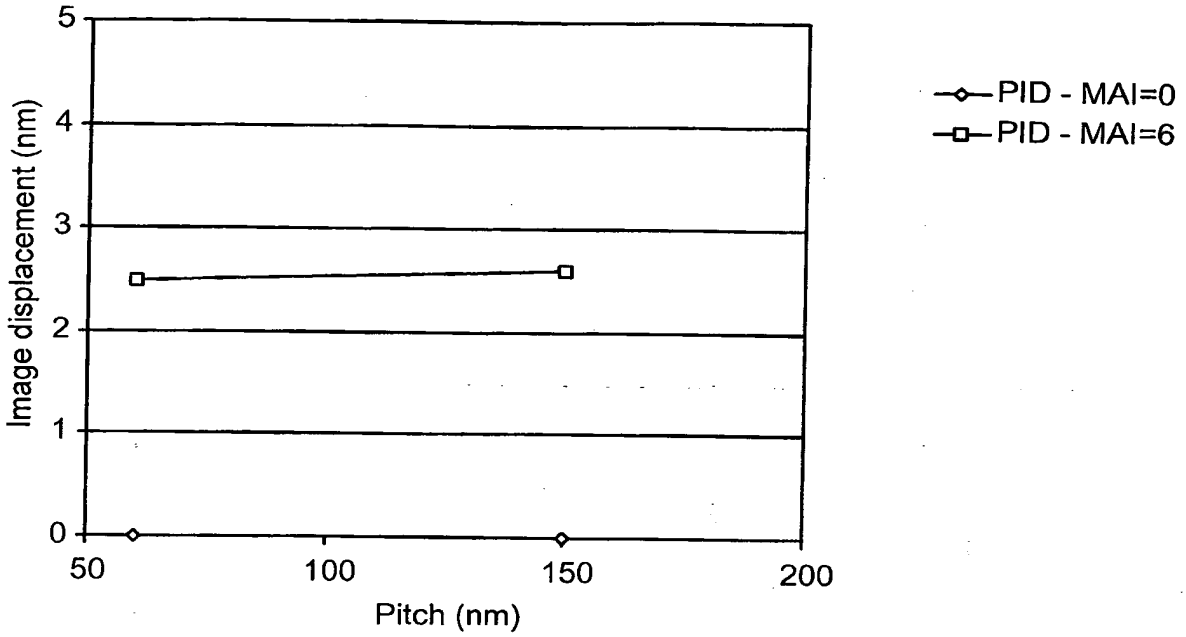
5
4
3
2
1
0
Image displacement (nm)
50
100
150
200
Pitch (nm)
PID - MAI=0
PID - MAI=6